Available online at www.eccomasproceedia.org
Eccomas Proceedia COMPDYN (2023) 1660-1668

ECCOMAS
Proceedia

COMPDYN 2023
9th ECCOMAS Thematic Conference on
Computational Methods in Structural Dynamics and Earthquake Engineering
M. Papadrakakis, M. Fragiadakis (eds.)
Athens, Greece, 12-14 June 2023

PREDICTING THE UNIAXIAL COMPRESSIVE CAPACITY OF NON-STRENGTHENED AND FRP-STRENGTHENED MASONRY COLUMNS USING A FAST NUMERICAL APPROACH

Luis C.M. da Silva[1], **Gabriele Milani**[1], **and Ernesto Grande**[2]

[1]Politecnico di Milano
Department A.B.C., Piazza Leonardo da Vinci, 20133, Milan, Italy
e-mail: {luiscarlos.martinsdasilva,gabriele.milani }@polimi.it

[2] University Guglielmo Marconi
Department of Engineering Sciences, , 00193, Rome, Italy
e-mail: {name2,name3}@e-mail.address

Abstract. *The work addresses the retrofitting of masonry columns through jacketing with polymeric-based composites. The presented numerical procedure assumes a strain-based incremental formulation relying on equilibrium, compatibility, and kinematic equations and precluding a strenuous integration required by a Finite Element approach. The strength domain of brick units and mortar joints is bounded by a multi-surface yield criteria: Mohr-Coulomb criteria in shear, a compression cap and a Rankine tension cut-off. Failure of the FRP is governed by limited tensile strength. A brittle response is considered for the system constituents, with exception for mortar joints in which an elasto-plastic response with limited ductility is assumed. The numerical strategy is validated with data from several experimental campaigns, but also compared with existing approaches from literature and code-based formulas. A good agreement has been found and the main purpose achieved, i.e. to develop a strategy that is accurate and fast.*

Keywords: Masonry, FRP, FRCM, compression strength, numerical model, analytical model.

ISSN:2623-3347 Published by Eccomas Proceedia.
Peer-review under responsibility of the organizing committee of COMPDYN 2023.
doi: 10.7712/120123.10509.20508

1 INTRODUCTION

The employment of unreinforced masonry in structural elements is generally limited due to its low tensile strength and quasi-brittle response. This behaviour has led to its predominant use in elements governed by compressive stresses [1, 2, 3]. Therefore, an accurate evaluation of the masonry's compressive strength is crucial for the design and assessment of the structural safety of buildings containing such materials. In order to estimate the compressive strength of masonry, the construction and testing of stacked masonry prisms or larger setups are commonly described in the literature [4], in accordance with European normative EN 1052-1 [5]. This data is crucial for the development of analytical strategies aimed at managing the costs associated with experimentation.

The compressive strength prediction of masonry is often a challenge due to the stress mismatch of the constituents [6, 7]. Although the behaviour of masonry under pure compression is well documented, the assessment of strengthened elements deserves more insight. The application of polymer-based jackets in load-bearing masonry elements allow to improve both strength and ductility [8, 9, 10, 11, 12, 13, 14, 15, 16, 17, 18, 19]. Experimental programs still are at a higher level when compared to the existing analytical and numerical tools of analysis [20]. The Italian normative [21] includes provisions formulated according to data from experiments on masonry elements, but the majority of the current literature stem from procedures originally oriented for concrete structures [22]. Accuracy of the predictions are thus dependent on ad-hoc calibrations to better correlate the results with the experimental data from different masonry types and thus have a limited scope [14, 15, 13, 23, 9]. This concern, together with the general discrepancies obtained when adopting current codes and literature formulations, has been recently raised [24]. The need of an analytical or numerical approach that provides accurate predictions of masonry columns reinforced with a polymeric-based wrapping, yet that is practical and provides immediate results, is lacking and has been highlighted in the literature [25, 24].

In such a context, the present research tries to address directly the need of a numerical tool to predict with accuracy the compressive strength of non-strengthened and strengthened squared columns made of periodic masonry. The type of strengthening accounted is that based on a polymeric composite through jacketing or wrapping, such as FRP (fiber reinforced polymer) based or TRM (textile reinforced mortar) based. A brief description of the strategy is addressed next, together with some preliminary results.

2 GENERAL SPECIFICATIONS

Hilsdorf research shed light on the fundamental mechanism underlying masonry compression failure. Under compression, the bed mortar joints tend to expand laterally, but the less deformable units restrict such lateral expansion. This gives rise to a state of pure tri-axial compression in the mortar joints and a state of compression-tension-tension in brick units, as depicted in Figure 1.

An elasto-plastic representative volume element (RVE) that occupies a domain $\Omega \in \mathbb{R}^3$ at initial time t_0 is considered for the modelling of a periodic type of masonry that represents a squared column under uni-axial compression. The formulation is provided in terms of principal strain and stress quantities. Using *Voigt's* notation, the generalized stress and strain components are given as $\sigma = [\sigma_1,\ \sigma_2,\ \sigma_3]$ and $\varepsilon = [\varepsilon_1,\ \varepsilon_2,\ \varepsilon_3]$, respectively. The RVE of the unit cell is modelled through a stack-bond approach (Figure 1), thence neglecting the effect of potential head joints. Geometric parameters serve directly as input for the formulation. For the sake of

readiness, it is indicated hereafter that $\sigma_1 = \sigma_v$, $\sigma_2 = \sigma_3 = \sigma_h$, in which the subscript v and h refers to vertical and horizontal directions, respectively.

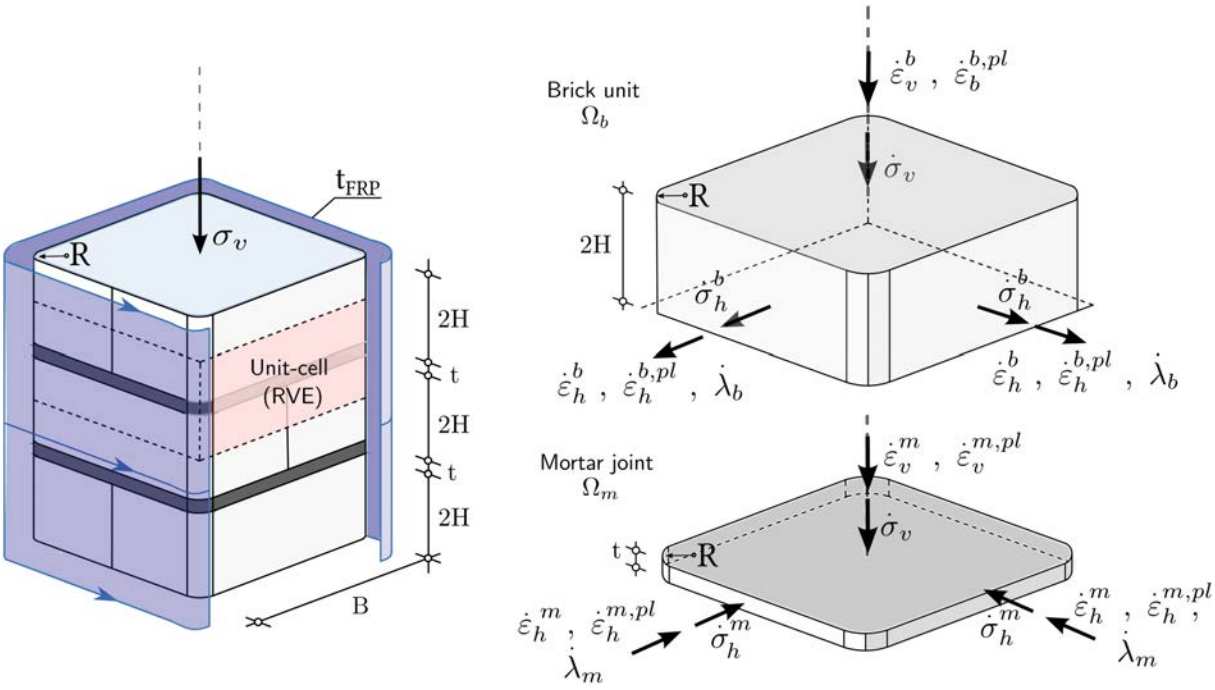

Figure 1: Squared unreinforced masonry column: geometry and stress state in the masonry components.

An incremental approach is pursued in which the stress state σ is evaluated for both mortar (Ω_m) and brick (Ω_b) constituents at each time increment t_k. The time variable t controls the prescribed increment of vertical strain $\Delta\varepsilon_v$ applied to the top surface boundary, which is established and assumed as known at the beginning of each *k* increment. Although ε:=$\varepsilon(t)$ and σ:=$\sigma(t)$, these are considered to be equal at any point $P \in \Omega_m$ and $P \in \Omega_b$ for a given time increment t_k. Strain vector is computed assuming an additive decomposition of the elastic ε_i^e and plastic ε_i^{pl} parts of strain. Accordingly, the strain variation for each increment k is found as:

$$\Delta\varepsilon_i^{(\cdot)} = \Delta\varepsilon_i^{(\cdot),e} + \Delta\varepsilon_i^{(\cdot),pl} \quad , \quad (\cdot) = m, b \ , \ \ i = v, h \tag{1}$$

in which the elastic increment $\Delta\varepsilon_i^{(\cdot),e}$ is determined according to a constitutive relationship based on the $Hooke's$ law. In specific, the time-independent relation for brick units is given in Equation (2) and written according to the corresponding Young's modulus E_b and Poisson's ratio ν_b. For mortar, the relation is given in Equation (3). The Young's modulus E_m is kept constant, but the Poisson's ratio can be defined by a time-dependent law $\nu_m(\sigma^m)$.

$$\varepsilon_k^{b,e} = [\Delta\varepsilon_h^{b,e} \ , \ \Delta\varepsilon_v^{b,e}]^T = \frac{1}{E_b}\begin{bmatrix} 1-\nu_b & -\nu_b \\ -2\nu_b & 1 \end{bmatrix}\begin{bmatrix} \Delta\sigma_h^b \\ \Delta\sigma_v^b \end{bmatrix} \tag{2}$$

$$\varepsilon_k^{m,e} = [\Delta\varepsilon_h^{m,e} \ , \ \Delta\varepsilon_v^{m,e}]^T = \frac{1}{E_m}\begin{bmatrix} 1-\nu_m(\sigma_{k-1}^m) & -\nu_m(\sigma_{k-1}^m) \\ -2\nu_m(\sigma_{k-1}^m) & 1 \end{bmatrix}\begin{bmatrix} \Delta\sigma_h^m \\ \Delta\sigma_v^m \end{bmatrix} \tag{3}$$

in which $\sigma_v^m = \sigma_v^b = \sigma_v$. The plastic strain increments are found by respecting the interface compatibility condition according to ***Hilsdorf's*** theory [6]. Strain equality is enforced in the horizontal direction in Equation (4) and vertical direction in Equation (5).

$$\Delta\varepsilon_h^{b,e} + \Delta\varepsilon_h^{b,pl} = \Delta\varepsilon_h^{m,e} + \Delta\varepsilon_h^{m,pl} \tag{4}$$

$$\Delta\varepsilon_v(2H+t) = 2H(\Delta\varepsilon_v^{b,e} + \Delta\varepsilon_v^{b,pl}) + t(\Delta\varepsilon_v^{m,e} + \Delta\varepsilon_v^{m,pl}) \tag{5}$$

The horizontal equilibrium is verified given the system components as:

$$2HB\Delta\sigma_{xx}^b + tB\Delta\sigma_{xx}^m = 0 \tag{6}$$

The admissible set of principal stresses is bounded by a closed and convex domain for both mortar and brick units. A multi-surface approach is adopted and provided in the $\sigma_1 - \sigma_3$ space under the condition that $\sigma_1 \leq \sigma_2 = \sigma_3$. A Mohr-Coulomb failure is adopted with a compression cap and a tension cut-off was adopted for both components.

At last, it is important to highlight the law that bounds the elastic nonlinear response of mortar. The proposed law follows the Ottosen [26] and the Mohamad [27] models. This is necessary to reproduce important phenomenological aspects related with the Poisson's ratio of mortar, such as: (1) its initial decrease, (2) the significant increase after the uni-axial compressive strength value, and (3) the rapid increase near failure which may reach very high values (range $\approx 0.8 - 0.9$) [28]. The inclusion of such internal variable is paramount to describe the non-linear elastic response of some mortars for higher confinement stresses.

$$\nu_k^m(\beta) = \begin{cases} 0.1 & \textit{if} \quad \beta \leq \beta_1 \\ \nu_m - (\nu_m - \nu_{inf})\sqrt{(1 - \frac{\beta-\beta_1}{1-\beta_1}} & \textit{if} \quad \beta_1 \leq \beta \leq 1.0 \\ \nu_m & \textit{if} \quad \beta \geq 1.0 \ \wedge \ f_m^{cap}(\sigma_k^m) < TOL_\sigma \\ 0.8 & \textit{if} \quad \beta \geq 1.0 \ \wedge \ f_m^{cap}(\sigma_k^m) \geq TOL_\sigma \end{cases} \tag{7}$$

in which $\beta = \frac{\sigma_v}{f_{cm}}$, $\beta_1 = 0.8$ [26], $f_m^{cap}(\sigma_k^m)$ is the mortar compression cap function and TOL_σ a tolerance assumed as $0.5 f_{cm}$.

3 APPLICATION

The accuracy of the proposed numerical model is evaluated based on the experimental campaigns on squared masonry columns from Faella et al. [29]. Faella et. al works [29] gather tests on 28 clay-brick masonry squared columns confined by 1 or 2 layers of GFRP. The cross-sections range $380 \times 380 mm^2$ and to $250 \times 250 mm^2$. The masonry prisms were casted with weak mortar. It is considered for the Mohr-Coulomb criteria of mortar a $\phi_m = 25.3 deg.$.

The columns evaluated are made of clay masonry and include the so-called type A and type B[29]. The type A columns have a radius $R = 10$ mm and brick height of $H = 30$ mm. These have been strengthened with either one or two layers for the FRP (glass fibers) jacket, whose experimental properties are $E = 80700$ MPa and $f_{d,FRP} = 2560$ MPa and for which the thickness of a single layer is defined as $t_{FRP} = 0.48$ mm.

The columns made of clay masonry type B have a radius $R = 25$ mm and brick height of $H = 55$ mm. These have been strengthened with either one or two layers for the FRP (glass fibers) jacket, whose experimental properties are $E = 65000$ MPa and $f_{d,FRP} = 1600$ MPa and for which the thickness of a single layer is defined as $t_{FRP} = 0.23$ mm. The squared column geometry changes either between a $B = 250$mm and $B = 380$mm.

The predicted results are compared in terms of ultimate capacity for both non-strengthened and strengthened cases, and values retrieved from the expressions of Eurocode 6 [30], ACI [22], Italian code [21] and results from Corradi et al. [13] are also presented. As input for mortar, it has been considered a $f_{cm} = 1.027$ MPa, $f_{tb} = 0.10 f_{cb}$ MPa, $E_m = 1000$ MPa (value suggested for lime-based mortar in [31]) and $\nu_m = 0.3$. For clay bricks of type A and following the interval proposed in [29], a $f_{cb} = 20.0$ MPa, $f_{tb} = 0.10 f_{cb}$ MPa, $E_b = 20000$ MPa (value found as $1000 f_c b$ [31]) and $\nu_b = 0.15$. For clay bricks of type B and following the interval proposed in [29], a $f_{cb} = 15.0$ MPa, $f_{tb} = 0.10 f_{cb}$ MPa, $E_b = 15000$ MPa (value found as $1000 f_c b$ [31]) and $\nu_b = 0.15$.

Results are presented in Figure 2. The proposed model proves to be accurate considering the different geometries of the column and strengthening options, such as wrapping nature, number and thickness of polymer-base layers. The numerical approach requires only 1 second of analysis since few increment of vertical strain are needed to achieve a solution. More importantly, it requires few input parameters that are typically retrieved from experimental material characterization tests.

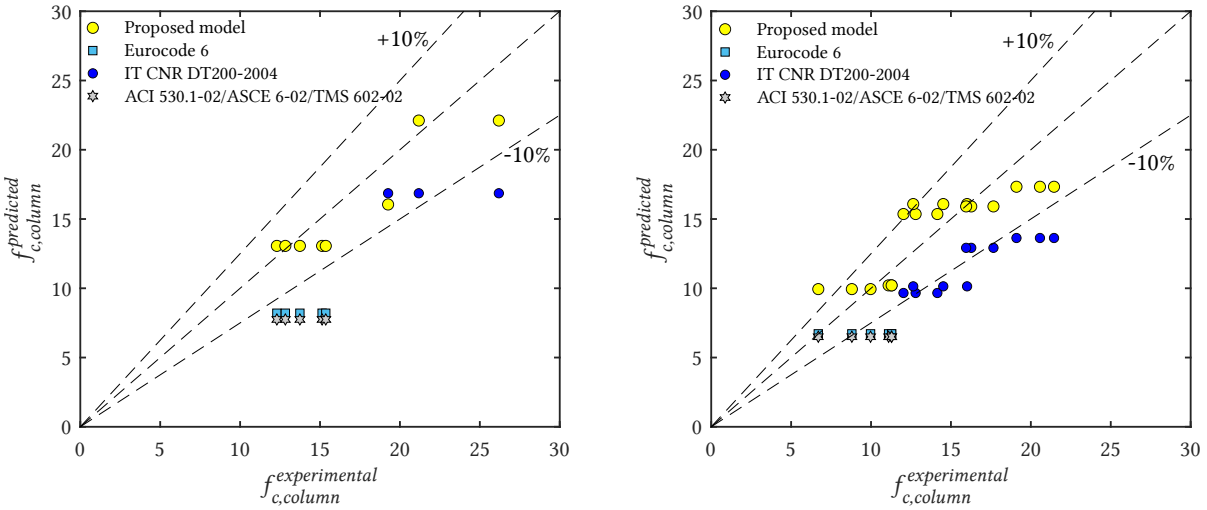

(a) clay masonry type A

(a) clay masonry type B

Figure 2: Comparison between the numerical and analytical predictions with the experimental data.

4 CONCLUSIONS

A fast numerical model was presented to predict the compressive strength of squared columns made of periodic clay brick masonry. The predicted values are within 10% difference with experimental data. It is rather evident that current normative strategies show, as intended, a conservative nature. Although the model seems promising, it is addressed that more experimental data are required for a further evaluation on its validity. The present study includes only data related to clay masonry and for a weak mortar. Further studies will demonstrate the suitability of the model on other types of masonry units and also in presence of strong mortars.

References

[1] P. B. Lourenço, L. C. Silva, Computational applications in masonry structures: from the meso-scale to the super-large/super-complex, International Journal for Multiscale Com-

putational Engineering 18 (1) (2020) 1–30. doi:10.1615/IntJMultCompEng.2020030889.

[2] M. F. Funari, L. C. Silva, E. Mousavian, P. B. Lourenço, Real-time Structural Stability of Domes through Limit Analysis: Application to St. Peter's Dome, International Journal of Architectural Heritage (2021) 1–23doi:10.1080/15583058.2021.1992539.
URL https://doi.org/10.1080/15583058.2021.1992539

[3] M. F. Funari, L. C. Silva, N. Savalle, P. B. Lourenço, A concurrent micro/macro FE-model optimized with a limit analysis tool for the assessment of dry-joint masonry structures, International Journal for Multiscale Computational Engineering 20 (5) (2022) 65–85. doi:10.1615/IntJMultCompEng.2021040212.

[4] N. Mojsilović, Strength of masonry subjected to in-plane loading: A contribution, International Journal of Solids and Structures 48 (6) (2011) 865–873. doi:https://doi.org/10.1016/j.ijsolstr.2010.11.019.
URL https://www.sciencedirect.com/science/article/pii/S002076831000418X

[5] CEN, En 1052-3: Methods of test for masonry–part 3: Determination of initial shear strength, European Committee for Standardization (2007).

[6] H. K. Hilsdorf, Investigation into the failure mechanism of brick masonry loaded in axial compression. Designing, engineering and constructing with masonry products, Gulf Publishing Company (1969) 34–41.

[7] C. Khoo, A. Hendry, A failure criterion for brickwork in axial compression, in: Proceeding of the 3rd International Brick/Block Masonry Conference, Essen, Germany, 1973, pp. 139–145.

[8] Y. Yuan, G. Milani, Closed-form model for curved brittle substrates reinforced with frp strips, Composite Structures 304 (2023) 116443. doi:https://doi.org/10.1016/j.compstruct.2022.116443.
URL https://www.sciencedirect.com/science/article/pii/S0263822322011758

[9] G. Minafò, J. D'Anna, C. Cucchiara, A. Monaco, L. La Mendola, Analytical stress-strain law of frp confined masonry in compression: Literature review and design provisions, Composites Part B: Engineering 115 (2017) 160–169, composite lattices and multiscale innovative materials and structures. doi:https://doi.org/10.1016/j.compositesb.2016.10.019.
URL https://www.sciencedirect.com/science/article/pii/S1359836816322144

[10] E. Grande, M. Imbimbo, E. Sacco, Finite element analysis of masonry panels strengthened with frps, Composites Part B: Engineering 45 (1) (2013) 1296–1309. doi:https://doi.org/10.1016/j.compositesb.2012.09.002.
URL https://www.sciencedirect.com/science/article/pii/S135983681200532X

[11] E. Grande, M. Imbimbo, E. Sacco, Bond behaviour of cfrp laminates glued on clay bricks: Experimental and numerical study, Composites Part B: Engineering 42 (2) (2011) 330–340. doi:https://doi.org/10.1016/j.compositesb.2010.09.020.

[12] T. C. Triantafillou, Strengthening of masonry structures using epoxy-bonded frp laminates, Journal of Composites for Construction 2 (2) (1998) 96–104. doi:10.1061/(ASCE)1090-0268(1998)2:2(96).

[13] M. Corradi, A. Grazini, A. Borri, Confinement of brick masonry columns with CFRP materials, Composites Science and Technology 67 (9) (2007) 1772–1783. doi:https://doi.org/10.1016/j.compscitech.2006.11.002.
URL https://www.sciencedirect.com/science/article/pii/S0266353806004246

[14] T. D. Krevaikas, T. C. Triantafillou, Masonry Confinement with Fiber-Reinforced Polymers, Journal of Composites for Construction 9 (2) (2005) 128–135. doi:10.1061/(ASCE)1090-0268(2005)9:2(128).
URL https://doi.org/10.1061/(ASCE)1090-0268(2005)9:2(128)

[15] C. Faella, E. Martinelli, G. Camorani, M. A. Aiello, F. Micelli, E. Nigro, Masonry columns confined by composite materials: Design formulae, Composites Part B: Engineering 42 (4) (2011) 705–716. doi:https://doi.org/10.1016/j.compositesb.2011.02.024.

[16] D. L. Marco, D. Claudio, P. Andrea, M. Gaetano, FRP Confinement of Tuff and Clay Brick Columns: Experimental Study and Assessment of Analytical Models, Journal of Composites for Construction 14 (5) (2010) 583–596. doi:10.1061/(ASCE)CC.1943-5614.0000113.
URL https://doi.org/10.1061/(ASCE)CC.1943-5614.0000113

[17] A. M. Antonietta, M. Francesco, V. Luca, FRP Confinement of Square Masonry Columns, Journal of Composites for Construction 13 (2) (2009) 148–158. doi:10.1061/(ASCE)1090-0268(2009)13:2(148).
URL https://doi.org/10.1061/(ASCE)1090-0268(2009)13:2(148)

[18] A. Cascardi, F. Longo, F. Micelli, M. A. Aiello, Compressive strength of confined column with fiber reinforced mortar (frm): New design-oriented-models, Construction and Building Materials 156 (2017) 387–401. doi:https://doi.org/10.1016/j.conbuildmat.2017.09.004.
URL https://www.sciencedirect.com/science/article/pii/S0950061817318044

[19] G. Milani, Simple model with in-parallel elasto-fragile trusses to characterize debonding on frp-reinforced flat substrates, Composite Structures 296 (2022) 115874. doi:https://doi.org/10.1016/j.compstruct.2022.115874.
URL https://www.sciencedirect.com/science/article/pii/S0263822322006419

[20] J. Witzany, T. Čejka, R. Zigler, Failure mechanism of compressed short brick masonry columns confined with frp strips, Construction and Building Materials 63 (2014) 180–188.

doi:https://doi.org/10.1016/j.conbuildmat.2014.04.041.
URL https://www.sciencedirect.com/science/article/pii/S0950061814003584

[21] CNR-DT200 R1/2013, Guide for design and construction of externally bonded FRP systems for strengthening existing structures: materials, RC and PC structures, masonry structures., Consiglio nazionale delle ricerche, 2013.

[22] ACI 440.2R-02, Guide for the Design and Construction of Externally Bonded FRP Systems for Strengthening Concrete Structures, American Concrete Institute, 2008. doi:10.1061/40753(171)159.

[23] G. P. Lignola, R. Angiuli, A. Prota, M. A. Aiello, FRP confinement of masonry: analytical modeling, Materials and Structures 47 (12) (2014) 2101–2115. doi:10.1617/s11527-014-0323-6.
URL https://doi.org/10.1617/s11527-014-0323-6

[24] A. Napoli, R. Realfonzo, Compressive behavior of masonry columns confined with frcm systems: Research overview and analytical proposals, Journal of Composites for Construction 26 (3) (2022) 04022019. doi:10.1061/(ASCE)CC.1943-5614.0001200.

[25] J. Thamboo, Performance of masonry columns confined with composites under axial compression: A state-of-the-art review, Construction and Building Materials 274 (2021) 121791. doi:https://doi.org/10.1016/j.conbuildmat.2020.121791.
URL https://www.sciencedirect.com/science/article/pii/S0950061820337958

[26] N. S. Ottosen, Constitutive model for short-time loading of concrete, Journal of the Engineering Mechanics Division 105 (1) (1979) 127–141. arXiv:https://ascelibrary.org/doi/pdf/10.1061/JMCEA3.0002446, doi:10.1061/JMCEA3.0002446.
URL https://ascelibrary.org/doi/abs/10.1061/JMCEA3.0002446

[27] G. Mohamad, F. S. Fonseca, H. R. Roman, A. T. Vermeltfoort, E. Rizzatti, Behavior of mortar under multitaxial stress, in: Proceedings of the 12th North American Masonry Conference, Denver, no. May, Denver, Colorado, 2015, pp. 17–20.

[28] C. S. Barbosa, P. B. Lourenço, G. Mohamad, J. B. Hanai, Triaxial compression tests on bedding mortar samples looking at confinement effect analysis, in: 10th North American Masonry Conference, St. Louis, Missouri, USA, pp. 1010–1020.
URL http://repositorium.sdum.uminho.pt/handle/1822/9199

[29] C. Faella, E. Martinelli, S. Paciello, G. Camorani, M. A. Aiello, F. Micelli, E. Nigro, Masonry columns confined by composite materials: Experimental investigation, Composites Part B: Engineering 42 (4) (2011) 692–704. doi:https://doi.org/10.1016/j.compositesb.2011.02.001.
URL https://www.sciencedirect.com/science/article/pii/S1359836811000746

[30] EN 1996-1-1, Eurocode 6: design of masonry structures. Part 1–1: general rules for reinforced and unreinforced masonry structures (2005).

[31] P. B. Lourenco, A. Gaetani, Finite Element Analysis for Building Assessment: Advanced Use and Practical Recommendations, Taylor & Francis, 2022.